Journal of Applied Mechanics and Technical Physics, Vol. 37, No. 4, 1996

MC-GENERATOR WITH A SHOCK-WAVE CASCADE

A. M. Trubachev and A. M. Ryabchun

UDC 537.639

In shock-wave MC-generators [1–3], the magnetic flux is compressed by shock waves, which transform nonconducting material into a conducting state. This method of megagauss magnetic field generation has certain advantages over liner devices. The technique of introducing the initial magnetic flux in the compression area is simplified. The problem of safety of the working volume is solved automatically. The initial shape of the compression area bounded by shock waves should be symmetrical, but this symmetry is not necessarily circular, which simplifies the explosive system.

Pavlovskii et al. [4] have studied the dynamics of collapse of the MC-generator shell. It has been shown that distortion of the compression symmetry of the shell and of the jet material evaporating from the liner surface causes premature sensor failure and, hence, a decrease in the maximum registered field. These phenomena were effectively inhibited by intermediate cascades [5], and the limiting field were increased [6, 7]. In our opinion, cascade MC and shock-wave generators have much in common and differ only in the material distribution over the compressed volume.

In the present paper, we discuss the attainment of maximum magnetic fields in a MC-generator with a shock-wave cascade. The problem of obtaining a maximum field in a given volume with a fixed initial kinetic energy of the liner which initiates a shock wave in the material filling the compression area is solved by selecting the generator's parameters.

1. When a MC-1 generator is used to produce megagauss magnetic fields, only two parameters (initial magnetic field and the size of the measuring unit) remain free after the explosive system is selected. Here and below, the notion of the size of the measuring unit implies not simply the cross-sectional dimensions of the field sensor or of the experimental device with protection, which are located on the axis, but a certain cross-sectional dimension of the compression area at the end of signal recording. In MC-1 generators, this dimension is primarily determined by the departure of the compressed shell from circular symmetry and is always greater than the geometrical dimensions of the measuring unit itself.

In shock-wave MC-generators, there is an additional degree of freedom, i.e., one can select the parameters of the compressed medium. The type of material and its initial density ρ_0 govern the shock-wave properties of the medium, and a variation of the initial-density distribution over the generator radius makes it possible to control (to a certain degree) the effectiveness of operation of the generator.

As is noted in [2, 8], the initial conditions and the current size of the compression area being the same, the field in the shock-wave generator appears to be smaller than that in a generator with a liner, because part of the flux is carried over by the matter through the wave front. For the same reason, at the end of compression the field in shock-wave generators is higher but has a smaller size.

It may appear that the same result would be obtained with a liner system by a reduction in the initial field. However, processing of the experimental data of [9] shows that only in unique cases [10] can one compress a liner by approximately 14-fold and amplify the field by a factor of 200 at the end of signal recording. The above restrictions are due to intense electrophysical processes that occur on the inner surface of the liner and necessitate stringent requirements for the protection of the measuring unit [4].

Shock-wave generators are practically free of these shortcomings. In the experiments of [11, 12], which were performed in the simplest setup, the size of the compression area varied by approximately a factor of

Lavrent'ev Institute of Hydrodynamics, Siberian Division, Russian Academy of Sciences, Novosibirsk 630090. Translated from Prikladnaya Mekhanika i Tekhnicheskaya Fizika, Vol. 37, No. 4, pp. 15–21, July–August, 1996. Original article submitted March 27, 1995.

40 from the moment of sensor failure and was determined only by the accuracy of focusing of shock waves on the sensor. The field sensor located on the generator axis was not protected except for electric insulation. Protection was provided by the working material itself. In the shock-wave generator, instabilities are probably strongly suppressed by the convective mixing of the field with the material and by the formation of a current layer of significant thickness. This can be inferred by the x-ray photographs of [4], taking into account the resemblance between the two types of generators.

Thus, the shock-wave generator outperforms the classical MC-generator in the degree of protection of the measuring unit. It also offers advantages in the density of magnetic energy at the end of operation, but the total energy in the compressed volume is smaller.

The advantages of the two systems can be combined if the compressible volume is filled with the working material only partially. Then, in the first stages, the generator operates as the classical generator with a high coefficient of conversion of the kinetic energy of the liner to magnetic energy, and, in the late stages, as a shock-wave generator.

2. Let us consider an axisymmetric problem of compression of the magnetic field in a MC-generator with a shock-wave cascade. A cylindrical region with radius r_0 and axial magnetic field B_0 is filled with a nonconducting material with initial density $\rho_0(r)$. A liner with mass M per unit length, inside radius r_0, and material density ρ_l compresses the medium with initial velocity u_0. A cylindrical shock wave that leaves the liner converts the medium into a conducting state and compresses the magnetic field.

We further assume the following conditions which simplify the problem: a) the liner and the shock wave converge symmetrically to the center; b) the medium–liner interface is continuous; c) the liner material is incompressible; d) the medium is packed by the shock wave from density $\rho_0(r)$ to uniform density ρ, which is then unchanged; e) the conductivity of the working medium appears only after its complete compression in the SW; and f) the diffusion losses of the flow from the compression area can be ignored over a wide range of the problem parameters [8]. With allowance for these remarks, the field in the compression area depends only on the area size:

$$b = \exp\Big(-2\int_1^{x_f} \alpha(x)/x\,dx\Big). \tag{2.1}$$

Here $x = r/r_0$ is the coordinate; $x_f = r_f/r_0$ is the position of the shock-wave front; $b = B/B_0$ is the field in the compression area; $\alpha(x) = 1 - \rho_0(x)/\rho = u/D$; and u and D are the mass and wave velocities in the shock wave.

For $\alpha =$ const, the field (2.1) coincides with the result of [2]; for $\alpha = 1$, with the classical limit $b = x_f^{-2}$.

The equation of motion of the wave front is obtained from the Euler equation by integration over the radius with a zero pressure on the outer boundary of the liner, with pressure $p_f = \rho_0(x_f)uD + B^2/(2\mu_0)$ at the shock-wave front, from the condition of continuity of the flow at the medium–liner interface and is of the form

$$v_f^2 = \frac{\rho_l}{\rho}\frac{w}{x_f^2}\frac{\ln(1+m)}{\ln((x_l/x_f)^2(1+m/x_l)^{\rho_l/\rho})}, \tag{2.2}$$

where w is an auxiliary function:

$$\frac{dw}{dx_f} = \frac{2}{x_f}\Big\{\frac{b^2\alpha(x_f)}{\varepsilon} + \frac{w[1-\alpha(x_f)]}{\ln((x_l/x_f)^2(1+m/x_l)^{\rho_l/\rho})}\Big\};$$

$$x_l^2 = 1 + 2\int_1^{x_f}\alpha(x)x\,dx; \tag{2.3}$$

$v_f = u_f/u_0$ is the mass velocity at the wave front; $x_l = r_l/r_0$ is the position of the inner boundary of the liner; $m = M/(\pi r_0^2\rho_l)$; and $\varepsilon = \varepsilon_{k0}/\varepsilon_{m0} = [\mu_0\rho_l u_0^2\ln(1+m)]/B_0^2$ is the ratio of the kinetic energy of the liner ε_{k0} to the magnetic energy ε_{m0} at the beginning of compression.

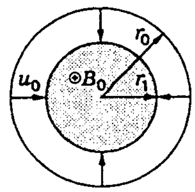

Fig. 1

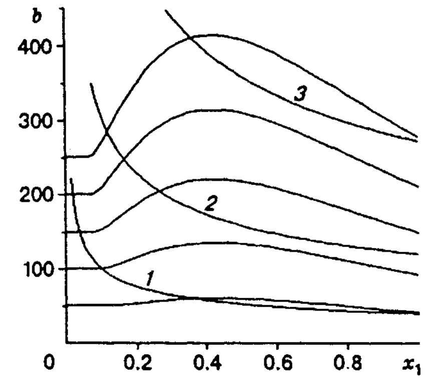

Fig. 2

TABLE 1

r_0, mm	M, kg/m	u_0, km/sec	ε_{k0}, J/m	ε_{m0}, J/m	B_0, T	B, T	B/B_0	$\varepsilon+1$	B_0^*, T	B^*, T	References
126	5.1	2.1	10^7	$8\cdot10^4$	4	360	90	125	3.5–4.5	700	[11, 12]
139	9	4.0	$8\cdot10^7$	—	5–100.16	500–1300	50–190	—	9–12	1800	[4–7]
147	6.2	1.54	$0.72\cdot10^7$	$5.2\cdot10^4$	2.78	323	116	138	3	500	[13]

3. The stated problem differs from that formulated in [8] by the character of material distribution in the compression area $\rho_0 = \rho_0(r)$. In principle, by selecting this distribution one can control (to a certain extent) both the shape of the magnetic-field pulse and the heat release in the layer compressing the field. However, we shall assume that the initial material density ρ_0 is constant for $r < r_1$ and $\rho_0 = 0$ for $r_1 < r < r_0$, since the specified distribution is simply realized in practice (Fig. 1).

The numerical calculations were carried out for a shock-wave generator [11, 12] whose characteristics are given in Table 1. The initial parameters of problem (2.1)–(2.3) such as m, r_0, ε, etc. are specified at the moment the detonation of an explosive charge terminates and are varied in the calculations in the vicinity of values typical of the generator [11, 12].

Figure 2 gives the calculation results for the amplification coefficient of the magnetic field $b = B/B_0$ for various values of the parameter ε. The horizontal axis $x_1 = r_1/r_0$ is the factor of filling of the generator's compression area by the working material ($x_1 = 1$ corresponds to the complete filling of the compression area by the porous material). The working material is PAP-1 aluminum powder with density $\rho_0 = 0.44$ g/cm^3.

The family of amplification curves is constructed 50 units apart starting with $\varepsilon = 50$. The amplification coefficient reaches a maximum at $x_1 = 0.4$–0.5 and its position depends only slightly on ε. The relative value of the maximum increases with increasing ε.

As x_1 decreases, the amplification is reduced and the curves enter a horizontal section. This section describes the operation of the generator under ideal conditions, i.e., with conservation of the flux and energy. The liner does not reach the central area filled with the porous material, and $b = \varepsilon + 1$. The amplification is also reduced if the compression area is completely filled with the porous material.

The field amplification curves are constructed under the assumption that the shock wave is reflected from the field and the field reaches a maximum value. However, one should bear in mind that the size of the compression area may be unattainable in practice because of the finite dimensions of the measuring unit, or inaccurate focusing of shock waves on the axis of the system, and premature failure of the sensor. To take into account these factors, curves 1–3, which correspond to minimum compression areas of $0.1r_0$, $0.05r_0$, and $0.03r_0$, are drawn in Fig. 2. Thus, the working range of parameters is defined: $x_1 \cong 0.4$–0.5. The minimum

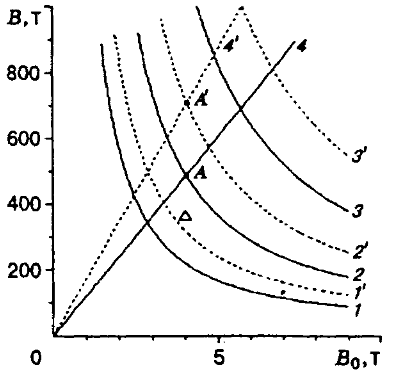

Fig. 3

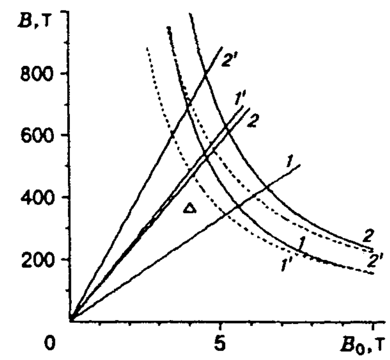

Fig. 4

size of the compression area depends on the design features, and the value of ε is selected so that the working point is located below the curve of the minimum size.

It is evident from Fig. 2 that for $\varepsilon > 100$ the field amplification can be higher by a factor of 1.5 and greater than that in the classical generator with a size acceptable for experiments (sensor $0.03r_0$–$0.05r_0$).

4. The representation of the data is convenient for choosing a part of the initial parameters of the generator irrespective of its design features. However, to determine the starting magnetic field and, hence, the final field in a particular situation, one should specify the kinetic energy of the liner at the beginning of compression.

Figure 3 gives the calculation results for the final magnetic field in the MC-generator as a function of the initial field for several values of the kinetic energy of the liner and various degrees of filling of the compression area by the porous medium. The solid curves correspond to the degree of filling $x_1 = 1$ and the dot curves, to $x_1 = 0.4$. Curves 1 and 1′ correspond to a liner energy of $0.5 \cdot 10^7$ J/m; curves 2 and 2′ to 10^7 J/m; and curves 3 and 3′ to $2 \cdot 10^7$ J/m. Along the curves the final field is amplified with a decrease in the initial field, but only as long as the final size of the compression zone remains greater than the size of the measuring unit. Violation of this condition results in premature failure of the sensor and the relationship between the initial and final fields is linear for various x_1 and is shown in Fig. 3 by straight lines 4 and 4′ which issue out from the coordinate origin. The size of the measuring unit is $0.05r_0$. The optimal magnetic field is determined by the point of intersection of the straight line and the curve of the corresponding energy. For the generator [11, 12] the optimal initial field is approximately 4 T irrespective of the degree of filling of the working area. The final magnetic field is $\approx$ 400–450 T for $x_1 = 1$ and $\approx$ 600–700 T for $x_1 = 0.4$ (points A and A').

To determine the influence of the other parameters on the final field, we performed a series of calculations with fixed liner energy and variable values of ρ_0 and m. Figure 4 shows the curve of the final field versus the initial field for various initial densities of the compressible material and various degrees of filling. Curves 1 and 1′, 2 and 2′ correspond to degrees of filling $x_1 = 1$ and 0.4. Curves 1′ and 2′ are plotted for density $\rho_0 = 0.44$ g/cm^3 while curves 1 and 2 are for a density greater by a factor of 1.5. The size of the sensor is always $0.05r_0$. The straight lines are marked by the same figures as the corresponding curves. One can see that with an increase in the initial density of the compressible material the field maximum decreases and is shifted toward greater initial fields.

In the experiments of [11, 12], the compression area was completely filled by an aluminum powder. The experiment result is shown by the triangle in Figs. 3 and 4. The closeness of the point to the corresponding boundaries indicates qualitative agreement between the experimental and calculation results. It is noteworthy, however, that the final magnetic field can be amplified approximately 2-fold only by selecting the optimal parameters of the shock-wave cascade, without changing the explosive system.

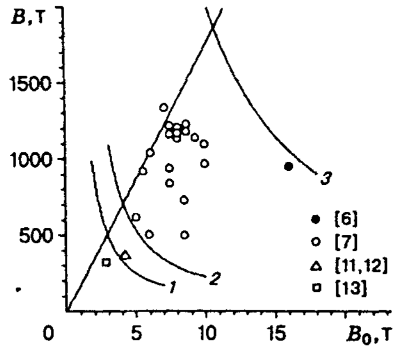

Fig. 5

5. The estimates obtained in Section 4 show that the use of a shock-wave cascade as the second stage of an MC-generator improves the operating characteristics of the latter such as the final field, and, taking into account the resemblance to the generator [4], the stability of results.

In this connection, it is of interest to estimate the gain in the final field that can be obtained if a shock-wave cascade is used in the well-known systems [4–7, 13].

Table 1 lists the parameters of the generators that were used to obtain megagauss magnetic fields.

It was additionally adopted in the calculations that the size of the cascade is $x_1 = 0.4$ and the filler is an aluminum powder with density $\rho_0 = 0.44$ g/cm^3. The size of the sensor is always $0.05r_0$. The calculation and the experiment results are presented in Fig. 5. Curve 1 refers to the generator from [13]; curve 2 from [11, 12], and curve 3 from [4–7]; the straight line is the line of the sensor. It is evident that in all three devices the final magnetic field can be amplified by means of a shock-wave cascade and optimal selection of the initial parameters of the generator. The required initial B_0^* and expected final B^* fields are given in Table 1.

In conclusion we note that it seems expedient to use a shock-wave cascade as the last stage of the classical MC-generator. The lower effectiveness of amplification of the cascade as compared with that of the liner device is compensated for by a longer time of signal recording. In the estimates we confined ourselves to a final compression area of $0.05r_0$, which is close to the values realized in [7, 13]. In fact, this size depends only on the accuracy of convergence of the shock wave to the system's axis, since the sensor does not require mechanical protection and can be as small as one likes; therefore, the calculated limit of attainable fields will be even higher. On the other hand, we used a shock adiabat of the compressible material that is different from the actual one. Allowance for the compressibility of the medium behind the shock-wave front decreases the limits of attainable fields. To take into account this factor and to ensure a certain safety margin, we confined ourself to the indicated final size of the compression area.

The authors are thankful to E. I. Bichenkov and S. D. Gilev for helpful remarks and advice.

This work was supported by the International Science Foundation (Grant RB0000) and the Russian Foundation for Fundamental Research (Grant 94-02-04022).

REFERENCES

1. Inventor's Certificate No. 762706, "Magnetocumulative generator (E. I. Bichenkov, N. G. Skorobogatykh, and A. M. Trubachev)," in: Otkr. Izobr., **1** (1982).
2. S. D. Gilev and A. M. Trubachev, "Generation of strong magnetic fields by shock waves in matter," *Pis'ma Zh. Teor. Fiz.*, **8**, No. 15, 914–917 (1982).
3. K. Nagayama, "New method of magnetic flux compression by means of the propagation of shock-induced metallic transition in semiconductors," *Appl. Phys. Let.*, **38**, No. 2, 109 (1981).
4. A. I. Pavlovskii, N. P. Kolokol'chikov, M. I. Dolotenko, et al., "Investigation of collapse dynamics of the shell of a magnetocumulative generator of ultrahigh magnetic fields," in: *Ultrahigh Magnetic*

Fields. Physics. Engineering. Applications: Proc. 3rd Int. Conf. on Generation of Megagauss Magnetic Field and Related Experiments, Novosibirsk, 1983, Nauka, Moscow (1984).

5. A. I. Pavlovskii, N. P. Kolokol'chikov, M. I. Dolotenko, et al., "Cascade magnetocumulative generator of multimegagauss magnetic fields," *ibid.*
6. A. I. Pavlovskii, N. P. Kolokol'chikov, O. M. Tatsenko, et al., "Reproducible generation of multimegagauss magnetic fields," in: *Megagauss Physics and Technology*: Proc. 2nd Int. Conf. on Megagauss Magnetic Field Generation and Related Topics, Washington, 1979, New York–London (1980).
7. A. I. Pavlovskii, A. I. Bykov, M. I. Dolotenko, et al., "Limiting value of reproducible magnetic field in cascade generator MC-1 ," in: *Megagauss Technology and Pulsed Power Applications*: Proc. 4th Int. Conf. on Megagauss Magnetic Field Generation and Related Topics, Santa Fe, 1986, New York–London (1987).
8. A. M. Trubachev, "Shock-wave MC-generators. Estimate of the limiting possibilities of the method," *Dynamics of Continuous Media* [in Russian], Institute of Hydrodynamics, Novosibirsk, **88** (1988), pp. 132–147.
9. A. M. Trubachev, "Effect of flux losses in MC-generator," in: *Megagauss Technology and Pulsed Power Applications*: Proc. 4th Int. Conf. on Megagauss Magnetic Field Generation and Related Topics, Santa Fe, 1986, New York–London (1987).
10. C. M. Fowler, W. B. Garn, and R. S. Caird, "Production of very high magnetic fields by implosion," *J. Appl. Phys.*, **31**, No. 3 (1960).
11. S. D. Gilev and A. M. Trubachev, "The use of shock waves for megagauss magnetic field generation," in: *Electromechanical Energy Converters* [in Russian], Naukova Dumka, Kiev (1986).
12. E. I. Bichenkov, S. D. Gilev, A. M. Ryabchun, et al., "Shock-wave method for generating megagauss magnetic fields," in: *Megagauss Technology and Pulsed Power Applications*: Proc. 4th Int. Conf. on Megagauss Magnetic Field Generation and Related Topics, Santa Fe, 1986, New York–London (1987).
13. T. Goto, N. Miura, K. Nakao, et al., "Megagauss field generation for application to solid state research," *ibid.*